Quantum adiabatic doping for atomic Fermi-Hubbard quantum simulations

Jue Nan,[1,2,3] Jian Lin,[2] Yuchen Luo,[2] Bo Zhao,[1,4,*] and Xiaopeng Li[2,5,†]

[1]*Hefei National Laboratory for Physical Sciences at Microscale and Department of Modern Physics, University of Science and Technology of China, Hefei, Anhui 230026, China*

[2]*State Key Laboratory of Surface Physics, Institute of Nanoelectronics and Quantum Computing, and Department of Physics, Fudan University, Shanghai 200433, China*

[3]*Shenzhen Institute for Quantum Science and Engineering, Southern University of Science and Technology, Shenzhen 518055, China*

[4]*Shanghai Branch, CAS Center for Excellence and Synergetic Innovation Center in Quantum Information and Quantum Physics, University of Science and Technology of China, Shanghai 201315, China*

[5]*Shanghai Qi Zhi Institute, Xuhui District, Shanghai 200032, China*

(Received 12 January 2021; accepted 25 March 2021; published 16 April 2021)

It is important to dope the antiferromagnetic state while preserving low entropy, in the quantum simulation of the Fermi-Hubbard model. In a recent work [Phys. Rev. Lett. **123**, 233603 (2019)], we proposed a quantum adiabatic doping protocol using an incommensurate lattice potential, where its feasibility is demonstrated with a certain particle-doping fraction. Here, we carry out a systematic study of quantum adiabatic doping for a wide range of doping fractions including both particle doping and hole doping, with both commensurate and incommensurate cases considered. We find that there is still a localizationlike slowing-down problem even at commensurate fillings, and that it becomes less harmful in the hole-doped regime. With interactions, the adiabatic preparation is found to be more efficient because the interaction effect destabilizes localization. For both free and interacting cases, we find adiabatic doping has a better performance in the hole-doped regime than the particle-doped regime. We also investigate adiabatic doping starting from a half-filling Mott insulator, which is found to be more efficient for certain filling fractions.

DOI: 10.1103/PhysRevA.103.043320

I. INTRODUCTION

Ultracold atoms in optical lattices provide a fascinating platform for quantum simulations of correlated many-body physics [1–4]. Since the atomic tunneling and interactions are both controllable in these systems, they have widely been used to study quantum many-body phases and quantum phase transitions. One main theme of quantum simulation with optical lattices is to investigate the low-temperature phase diagram of the Fermi-Hubbard model [5–7], and help uncover the fundamental mechanism of high-temperature superconductivity [8].

Whether and how d-wave superconductivity arises in the doped region including both hole- and particle-doped cases, in the repulsive Fermi-Hubbard model, has been attracting continuous research efforts [8–11], but this remains an open question with no consensus reached [10,11]. One reason is that numerical simulations on classical computers meet the fundamental challenges of exponentially growing Hilbert space of the quantum many-body system. This makes quantum simulations of the doped Fermi-Hubbard model very much in demand. With the development of ultracold-atom experiments, the low-temperature antiferromagnetic phase has now been reached at half filling [12–14]. The doping of an antiferromagnet with a hole has been realized by reducing the density of the trapped gases [14]. However, cooling down the system to a sufficiently low temperature in the doped regime, in order to simulate strongly correlated physics, is experimentally challenging. How to optimally perform doping for an atomic Fermi-Hubbard optical lattice system while maintaining low entropy of the system demands more theoretical study.

A plausible method to maintain a quantum simulator at low entropy is to perform quantum adiabatic doping. Adiabatic quantum state preparation has been widely applied in quantum state engineering and quantum simulations [15–21]. For the fermions confined in the optical lattice, a different filling factor is achieved by adiabatically converting a lattice with one spatial period to a lattice with a different period. Going through an adiabatic evolution from insulating states to the doped regime, the system remains at the ground state of the instantaneous Hamiltonian. This protocol has been studied to prepare a Fermi-Hubbard antiferromagnet insulating state [18,20], and also a doped ground state [15] with incommensurate fillings. For the incommensurate case, it has been found that the major difficulty in carrying out quantum adiabatic doping is from fermion localization [15]. The physics of fermion localization occurring in the intermediate dynamics prevents efficient state preparation, causing the problem of localization slowing down. Previous studies have established that repulsive interactions drive a generic tendency towards delocalization in interacting Aubry-André (AA) lattice models, as shown for both one- [22] and two-component fermions [15,23], as well as for bosons [24,25]. The interaction-driven

*bozhao@ustc.edu.cn
†xiaopeng_li@fudan.edu.cn

delocalization transition for the AA model has been observed in experiments with cold atoms [23,26–28]. In the case of random disorder, this transition has been observed with trapped ions [29], and superconducting qubits [30,31]. Therefore, we introduce an atomic interaction to solve the localization slowing down and it has been found to improve the preparation efficiency of adiabatic doping.

Since the focus of Ref. [15] is to show the feasibility of quantum adiabatic doping for incommensurate filling, only one filling factor at the particle-doped regime was studied. How the quantum adiabatic doping behaves for different fillings requires a more systematic study. In particular it is worth addressing whether the doping protocol remains efficient in the hole-doped regime. In this work we carry out a systematic study on quantum adiabatic doping in a one-dimensional optical lattice for a broad range of filling factors, with numerical simulations based on the time-dependent density-matrix renormalization group (DMRG) method.

We find that the localization slowing down is a generic problem for both commensurate and incommensurate fillings. For an incommensurate case, the localization problem is more fundamental because localization persists in the thermodynamic limit. This problem also causes slowing down for a commensurate case considering a finite-size system with a localization length significantly smaller than the system size, although it scales linearly with the system size in the thermodynamic limit. For particle doping, we show that adiabatic preparation efficiency can be enhanced by introducing an atomic interaction for both commensurate and incommensurate fillings. For hole doping, we find that the localization is much weaker, which we attribute to the large particle tunneling of the final lattice. Quantum adiabatic hole doping is consequently more efficient than particle doping, and efficiency can be further improved by including a strong atomic interaction. Besides starting from a band insulator, we also consider adiabatic particle doping starting from a Mott insulator at half filling. Our numerical simulation shows that quantum adiabatic doping starting from a Mott insulator has a better performance for certain fillings. We expect these numerical results on quantum adiabatic doping for a one-dimensional optical lattice would also shed light on a two-dimensional lattice.

II. THEORETICAL SETUP

The atomic quantum simulator of the Fermi-Hubbard model consists of two-component fermionic atoms confined in a periodical optical lattice. The system is described by the Hamiltonian

$$H = \int d^d\mathbf{x}\Bigg[\sum_\sigma \psi_\sigma^\dagger\left(-\frac{\hbar^2\nabla^2}{2M} + V(\mathbf{x}) - \mu\right)\psi_\sigma + g\psi_\uparrow^\dagger\psi_\downarrow^\dagger\psi_\downarrow\psi_\uparrow\Bigg], \tag{1}$$

where $\psi_{\sigma=\uparrow,\downarrow}(\mathbf{x})$ is the quantum field operator for the corresponding pseudospin (hyperfine state) $\uparrow$ and $\downarrow$ components, M the atomic mass, μ the chemical potential, g the interaction strength between the two components, and $V(\mathbf{x})$ the optical lattice potential. We neglect the harmonic potential in our calculation for simplicity. In this work we first consider a one-dimensional ($d = 1$) band insulator as the initial state of adiabatic evolution. In optical lattice experiments, band insulators with low entropy have been achieved [20]. The initial lattice potential reads as

$$V_I(x) = \mathcal{V}\cos(2\pi x/\lambda), \tag{2}$$

with λ the lattice constant and V the strength. Then we adiabatically convert the lattice to another one with a different period,

$$V_F(x) = \mathcal{V}'\cos(2\pi x/\lambda'). \tag{3}$$

During the time evolution, the potential has a time-dependent form

$$V(x,t) = [1 - s(t/T)]V_I(x) + s(t/T)V_F(x), \tag{4}$$

which is standard in the context of an adiabatic algorithm [32]. Here, we adopt a linear path for adiabatic evolution

$$s(t/T) = t/T, \tag{5}$$

with T the total evolution time. In the calculation, we focus on the parameter choice of $\mathcal{V} = \mathcal{V}'$, and examine the consequence of varying the overall lattice strength. Assuming that the atomic loss during the evolution is negligible, which holds when the evolution time T is smaller than the lifetime of the cold-atom system, the filling factor of the final state is $f = \lambda'/\lambda$. By controlling the ratio between the lattice constants, a generic filling factor is accessible with quantum adiabatic doping. To illustrate the adiabatic doping process, we show the time dependence of the lattice potential and time evolution of a density profile

$$n(t) = |\Psi(t)|^2 \tag{6}$$

of free fermions in the doping process in Fig. 1, with $T = 400\hbar/E_R$, $\mathcal{V} = 4E_R$, and $f = 1/3$.

With the incommensurate potential in Eq. (4), the quantum dynamics during adiabatic evolution cannot be described by a valid tight-binding model. We thus have to take into account the continuous degrees of freedom of the lattice. In the numerical simulation, we discretize the space as $x \to j \times a$, with a the length of a grid, and j the discrete index. The discretization of space leads to a lattice Hamiltonian

$$H = \sum_j\{-J[c_{j\sigma}^\dagger c_{j+1,\sigma} + \text{H.c.}] + V_j c_{j\sigma}^\dagger c_{j\sigma} + U n_{j\uparrow}n_{j\downarrow}\}, \tag{7}$$

with parameters $J = \hbar^2/(2Ma^2)$, $V_j = V(x = ja)$, and $U = g/a$.

To evaluate the performance of adiabatic doping, we calculate the wave-function overlap

$$\text{Overlap} = |\langle\Psi_g|\Psi(T)\rangle|, \tag{8}$$

and the residual energy

$$\Delta E = \langle\Psi(T)|H_F|\Psi(T)\rangle - \langle\Psi_g|H_F|\Psi_g\rangle, \tag{9}$$

where $|\Psi_g\rangle$ is the ground state of the final Hamiltonian H_F, and $|\Psi(T)\rangle$ is the final state of quantum adiabatic evolution.

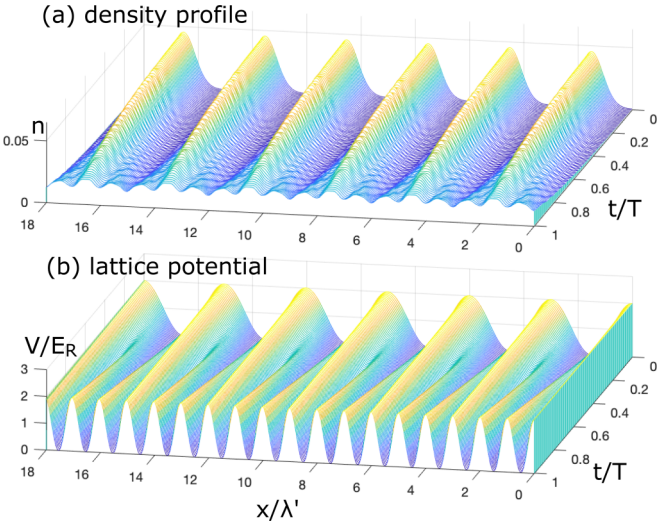

FIG. 1. The time evolution of a density profile [see Eq. (6)] of free fermions and a lattice potential [see Eq. (4)] in quantum adiabatic doping in one dimension with the potential strength $\mathcal{V} = 4E_R$ (E_R is the single-photon recoil energy) and total evolution time $T = 400\hbar/E_R$. The filling fraction is $f = 1/3$, corresponding to the hole-doped case. Here, λ' is the spatial period of the final lattice [see Eq. (3)].

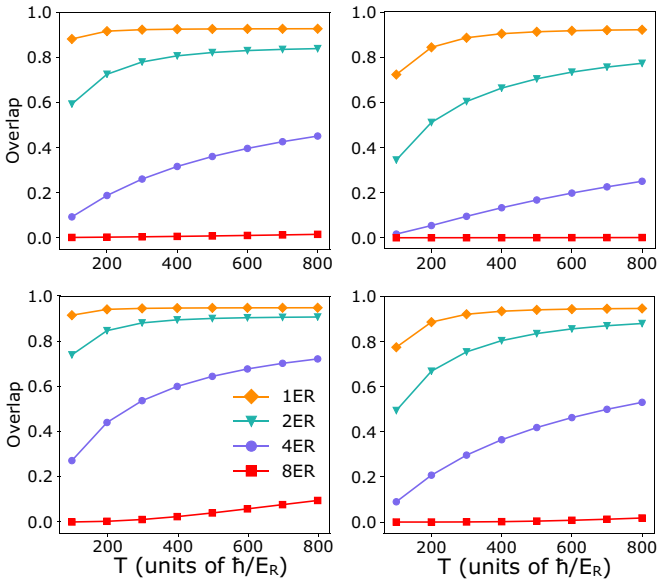

FIG. 2. The dependence of final-state wave-function overlap on total evolution time T for quantum adiabatic particle doping of free fermions in a one-dimensional lattice. We start from band-insulator states with the number of spatial periods $L = 36$ in (a), (c) and $L = 60$ in (b), (d). The resultant rational filling factors are $f = 3/4$ in (a), (b) and $f = 2/3$ in (c), (d). The wave-function overlap systematically increases with the adiabatic time T and approaches 1 as we increase the evolution time T for a weak lattice potential. For a stronger potential, the overlap remains nearly zero and the adiabatic doping protocol fails for free fermions.

To confirm our finding is generic for a finite-size system, we consider more than one system size in the following.

To simulate interacting fermions, we apply the standard DMRG to the discretized lattice model in Eq. (7). A second-order Trotterization is implemented in the time evolution [33]. This approach of simulating interacting systems in continuous space has also been previously used in the study of Fulde-Ferrell-Larkin-Ovchinnikov pairing of attractive fermions [34–36] and a Bose-Fermi mixture confined in a one-dimensional harmonic trap [37]. In the following calculation, we divide each spatial period of the initial lattice into 20 grids, if not specified. In our DMRG simulation, we have checked convergence with increasing the discretization grids (M) and the Trotterization steps (see the Appendix). The largest bond dimension of the time-dependent matrix product state used here is $D = 120$, for which numerical convergence is reached (see Ref. [15]).

III. PARTICLE DOPING

A. Free fermion

We first study the adiabatic particle doping of free fermions. This corresponds to setting the filling factor f larger than $1/2$. We simulate adiabatic evolution with rational filling factors $f = 2/3, 3/4$ and calculate the overlap of the final state with the ground state [Eq. (8)]. The dependence of the wave-function overlap on the total evolution time T is shown in Fig. 2. The initial state is a one-dimensional band insulator without an interaction in an optical lattice with L periods. We consider two different choices of system sizes, $L = 36$, and $L = 60$. For current and following calculations, we use a periodical boundary condition for noninteracting fermions, while the open boundary condition is adopted for the DMRG simulation of interacting fermions for numerical implementation convenience. For a weak lattice potential, say $\mathcal{V} = 1E_R, 2E_R$, the overlap increases with T and quickly approaches 1 as we increase the total evolution time. This implies the adiabatic preparation of the final state is efficient for weak lattice confinement. However, with a strong lattice potential ($\mathcal{V} = 8E_R$, for example), the final-state overlap essentially remains at zero for all evolution times we have simulated, which means the adiabatic doping is inefficient.

For adiabatic doping with an incommensurate lattice, the localization in the intermediate dynamics leads to a slowing down of adiabatic state evolution. This has been shown by the increase of the inverse participation ratio (IPR) [22,38–45] with the lattice potential strength [15]. In the commensurate case, similarly, the breakdown of adiabatic state preparation under strong lattice confinement indicates a localizationlike problem also occurs during evolution. To investigate the slowing-down problem in the commensurate lattice, we calculate the normalized participation ratio (NPR) [46]. The NPR of a single-particle eigenstate $\phi_m(x)$ is defined as

$$\mathrm{NPR}^{(m)} = \left[L \sum_j |\phi_m(j)|^4 \right]^{-1}, \tag{10}$$

where L is the system size, and j labels the discrete spatial coordinate [see Eq. (7)]. This quantity remains finite for spatial extended states but vanishes for localized states. For a one-dimensional localized system with length L, it goes as L^{-1}. We calculate the single-particle NPR of the lowest L

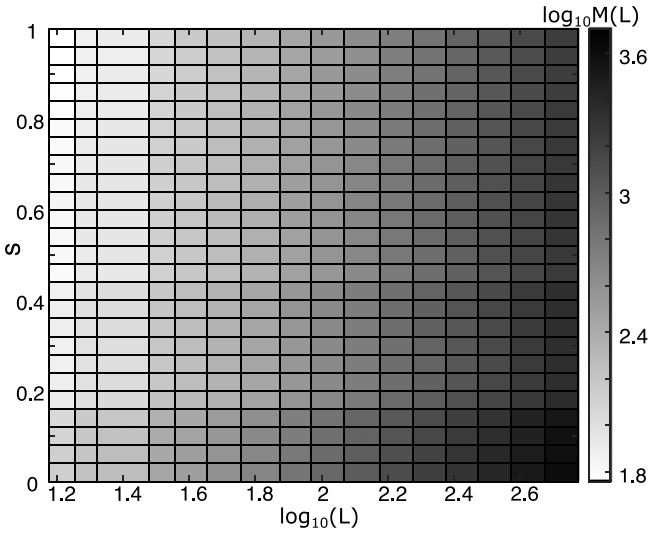

FIG. 3. The dependence of the quantity $\log_{10}M(L)$ [Eq. (12)] on L for the adiabatic particle doping of one-dimensional free fermions. Here, $s \in [0, 1]$ is the evolution path [Eq. (4)]. The system size L takes values from 15 to 597 with a rational filling factor $f = 2/3$. The potential strength is $\mathcal{V} = \mathcal{V}' = 8E_R$, for which the intermediate regime of evolution is strongly localized. At each instant s, $\log_{10}M(L)$ increases with L, which implies that the localization becomes unstable as the system becomes larger and tends to disappear in the thermodynamic limit. Nonetheless, the significant deviation of $M(L)$ from L for a finite-size lattice already implies the coupling between wave functions is rather weak, which affects the quantum adiabatic doping.

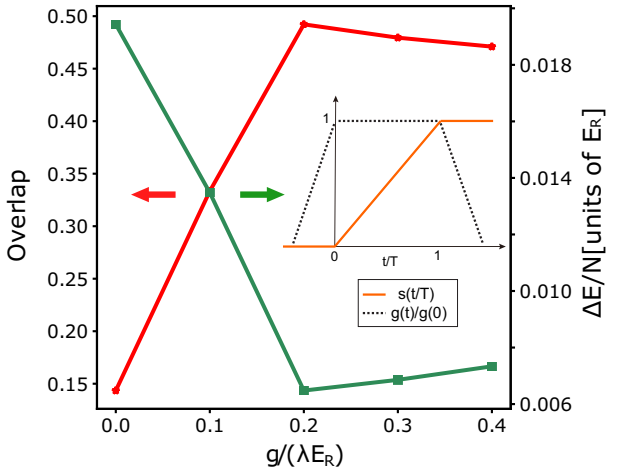

FIG. 4. Quantum adiabatic particle doping of one-dimensional interacting fermions. The interaction is adiabatically switched on for a one-dimensional noninteracting band insulator, held constant to implement the lattice conversion, and then adiabatically turned off, as shown by the inset. We perform a DMRG simulation of the lattice conversion process in the regime $t \in [0, T]$ with $T = 200\hbar/E_R$, taking the Hamiltonian in Eq. (7). The filling factor is chosen as $f = 2/3$ with $L = 14$ and $L' = 21$. The strength of the potential is $\mathcal{V} = 8E_R$. As we increase the interaction strength from $g = 0$ to $g = 0.2\lambda E_R$, the final-state wave-function overlap increases and the residual energy per particle $\Delta E/N$ (N is particle number) becomes smaller. The localization problem is reduced and the performance of the adiabatic doping is improved by introducing an interaction of proper strength.

eigenstates and average them to get

$$\langle \mathrm{NPR} \rangle = \frac{1}{L}\sum_{m=1}^{L} \mathrm{NPR}^{(m)}. \tag{11}$$

The averaged NPR is multiplied by L to compensate the L^{-1} scaling:

$$M(L) = L\langle \mathrm{NPR} \rangle. \tag{12}$$

Therefore, for a localized one-dimensional system, $M(L)$ is expected to be nearly independent of L. In Fig. 3 we show the dependence of the quantity $\log_{10}M(L)$ on L following the evolution path. The filling factor is set to be $f = 3/4$ and the overall potential strength is $\mathcal{V} = 8E_R$. It is evident that $M(L)$ increases quickly with L at each instant of the path. While this is consistent with the well-known fact that commensurate lattice models do not have localization in the thermodynamic limit, having a $\langle \mathrm{NPR} \rangle$ significantly smaller than 1 in a finite-size system implies the coupling between different modes is severely suppressed owing to the locality of the Hamiltonian, which then causes the slowing down of the quantum adiabatic evolution.

B. Interacting fermion

Localization makes the minimal energy gap between the ground state and the first excited state exponentially small, and therefore causes a slowing down of the adiabatic state preparation. It has been established that the interaction effect tends to destabilize localization, which would then improve the efficiency of the quantum adiabatic doping. This has been shown to be efficient for an incommensurate lattice with a strong interaction in Ref. [15]. In this work, we consider introducing a time-dependent interaction

$$H_{\mathrm{U}} = g(t)\int dx \psi_\uparrow^\dagger \psi_\downarrow^\dagger \psi_\downarrow \psi_\uparrow, \tag{13}$$

with the time sequence shown in the inset of Fig. 4. The system is initially prepared in a one-dimensional noninteracting band insulator with 14 periods. The interaction is turned on slowly and ramped to a constant. Then the initial optical lattice is adiabatically converted to another spatial period, after which the interaction is turned off slowly. The size of the final lattice is $L' = 21$, which corresponds to a rational filling factor $f = 2/3$. We simulate the lattice conversion process using DMRG. The total evolution time is $T = 200\ \hbar/E_R$ with 26 000 evolution steps. The wave-function overlap and the residual energy per particle at $t = T$ are shown as functions of the interaction strength g in Fig. 4. Here, the overall potential strength is $\mathcal{V} = 8E_R$, for which the noninteracting quantum adiabatic doping is inefficient. As we increase the interaction strength g from 0 to 0.2 (in units of λE_R with λ the initial lattice constant), the wave-function overlap is improved from 0.128 to 0.484, and the residual energy per particle $\Delta E/N$ (N is the number of particles) becomes very suppressed. We thus find that in the commensurate case, the slowing-down problem can still be solved by introducing an atomic interaction. A dramatic enhancement of the preparation efficiency is

achieved with a proper interaction strength. However, when we further increase the interaction strength, we find that the overlap decreases and $\Delta E/N$ increases slightly.

We also consider performing quantum adiabatic doping starting from a Mott insulating state. In experiments, such an initial state is accessible since low-temperature antiferromagnetic order has been observed at half filling in two-dimensional optical lattices [14]. To compare the performances of starting from the two different initial states of Mott and band insulators, we simulate the adiabatic lattice conversion starting from an interacting band insulator with L periods and a Mott insulator with $2L$ periods. We choose five different fillings in the particle-doped regime, both rational and irrational. Without loss of generality, the irrational filling factor is set to be the golden ratio, which is approximated by the Fibonacci sequence as $8/13$ and $13/21$ in our finite-size calculation. Here, we consider several different system sizes, $L = 8, 9, 12, 13$. For a Mott insulator, each period of the initial lattice is divided into ten grids, while that for a band insulator is divided into 20 grids. This parameter choice is chosen such that the final states of two protocols have the same spatial periods and discrete grids. The total evolution time is $T = 200\hbar/E_R$ for the smaller system of $L = 8, 9$ and $T = 200\hbar/E_R, 300\hbar/E_R, 400\hbar/E_R$ for the larger one of $L = 12, 13$. During the evolution, the interaction strength is held constant at $g = 0.4\lambda E_R$ and the overall potential strength takes the value $\mathcal{V} = \mathcal{V}' = 8E_R$. The final-state wave-function overlap is shown in Fig. 5 with the solid and dashed lines representing the results for the band insulator and Mott insulator, respectively. The overlap is larger for a band insulator at $f = 3/5$ and $f = (\sqrt{5}-1)/2$. For $f = 2/3$ and $3/4$, the adiabatic doping starting from a Mott insulator has a better performance. The advantage is especially evident for $f = 3/4$. As shown in Fig. 5(c), the overlap reaches 0.93 at $T = 300\hbar/E_R$ for a Mott insulator while that for a band insulator is 0.17. At $f = 4/5$, the overlaps of the two protocols are both smaller than $1/2$ for all adiabatic times we have simulated. As shown in Fig. 5(d), the overlap starting from a Mott insulator exceeds that of a band insulator and reaches 0.31 at $T = 400\hbar/E_R$. We expect the overall performance can be further improved by increasing the total evolution time.

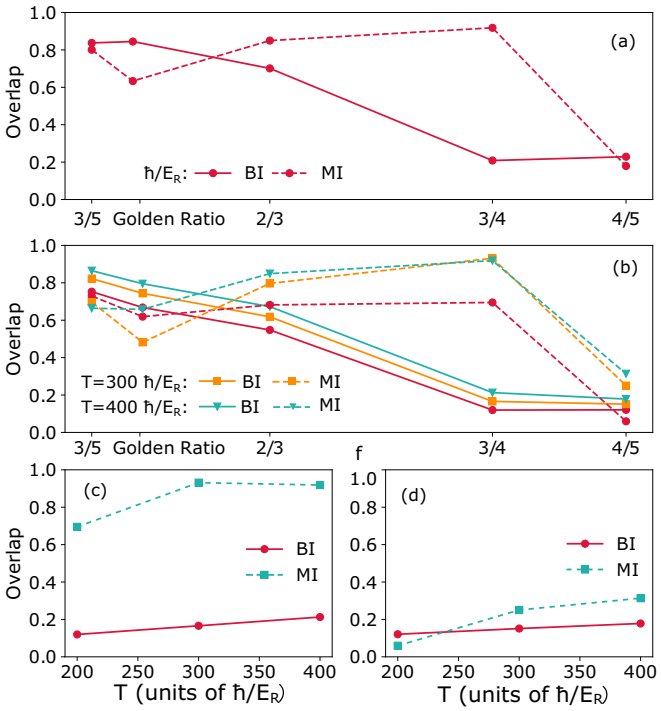

FIG. 5. Performance of quantum adiabatic doping of one-dimensional interacting fermions starting from a band insulator and Mott insulator. The doping process takes the time sequence as shown in Fig. 4 with $g = 0.4\lambda E_R$ and the DMRG simulation is performed in the regime $t \in [0, T]$. The number of spatial periods is L for a band insulator and $2L$ for a Mott insulator, corresponding to the lattice constant $\lambda/2$. The final-state wave-function overlaps of these two different protocols are compared in (a) for $L = 8, 9$ with the evolution time $T = 200\hbar/E_R$ and (b) for $L = 12, 13$ with $T = 200\hbar/E_R$, $300\hbar/E_R$, $400\hbar/E_R$. We choose five different final-state fillings, both rational and irrational. In (c) and (d), we show the dependence of the wave-function overlap on the adiabatic time T with $f = 3/4$ and $4/5$, respectively. For $f = 2/3$ and $3/4$, adiabatic doping starting from a Mott insulator has a better performance. The comparison is most dramatic for $f = 3/4$, as shown in (c). For $f = 4/5$, the wave-function overlaps of both procedures are smaller than $1/2$ in the time regime we consider. As we increase T, the protocol starting from a Mott insulator is more efficient than that from a band insulator.

IV. HOLE DOPING

A. Free fermion

In this section we study adiabatic hole doping, which corresponds to a filling factor smaller than $1/2$. We first simulate the adiabatic evolution of free fermions starting from a one-dimensional noninteracting band insulator in an optical lattice with L periods. Both rational and irrational fillings are considered. The rational filling factors are chosen as $f = 1/3, 1/4$, while for the irrational case we take $f = [3-\sqrt{5}]/2$, which is approximated by a Fibonacci sequence as $f = F_{n-2}/F_n$. We choose four different system sizes, $L = 36, 60$ for the rational fillings and $L = 34, 55$ for the irrational case. The dependence of the final-state wave-function overlap on the total evolution time is shown in Fig. 6. The overlap systemically increases with evolution time for all potential strengths we consider. It should be noticed that a wave-function overlap larger than $1/2$ can be reached for a larger system of $L = 55, 60$ with $\mathcal{V} = 8E_R$ and a smaller system of $L = 34, 36$ with $\mathcal{V} = 16E_R$ as we increase the evolution time to $T = 800\hbar/E_R$. The adiabatic doping remains efficient in the hole-doped regime even for moderate lattice potentials, for example, with $\mathcal{V} = 8E_R, 16E_R$, in contrast to the particle doping, which is severely subjected to the localization slowing-down problem. For a sufficiently strong lattice potential, the slowing-down problem still occurs in the quantum adiabatic evolution of the hole-doped case.

To investigate localization in the hole-doped regime, we calculate the inverse participation ratio (IPR), which tends to vanish in the extended system and remains finite in the localized system. The IPR is averaged over the lowest L single-particle eigenstates following the evolution path. The results are shown in Fig. 7. The irrational filling is set to be $f = [3-\sqrt{5}]/2$, which is approximated by $55/144$ with $L = 55$. The averaged IPR systematically increases with the

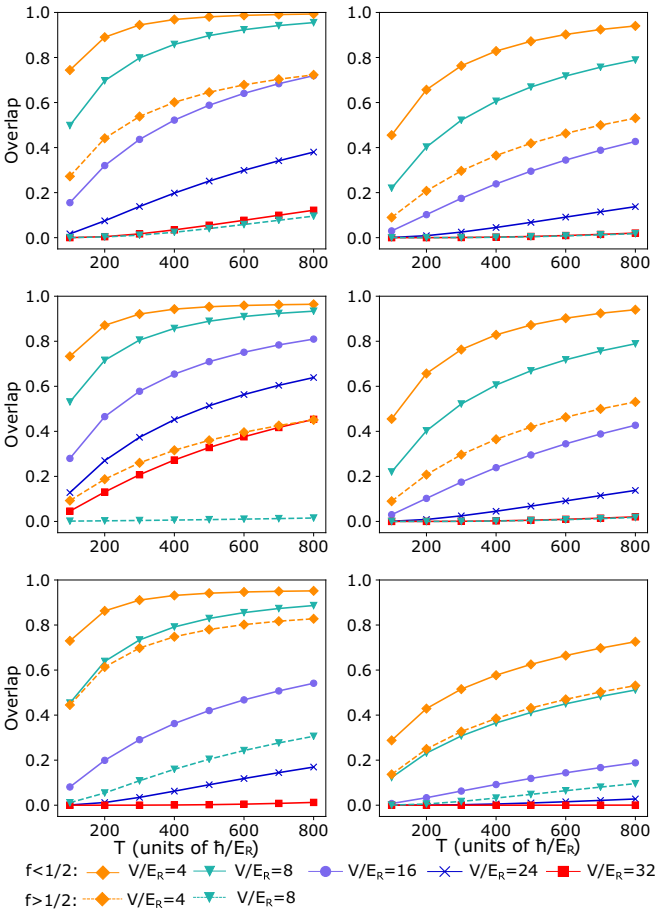

FIG. 6. The dependence of final-state wave-function overlap on evolution time T of adiabatic hole doping (solid lines) of free fermions in one dimension. For commensurate hole doping, the filling factors are set to be $f = 1/3$ in (a), (b) and $f = 1/4$ in (c), (d) with $L = 36$ (left) and $L = 60$ (right). It also takes an irrational value $[3 - \sqrt{5}]/2$, which is approximated by the Fibonacci sequence as $f = 34/89$ with $L = 34$ in (e) and $f = 55/144$ with $L = 55$ in (f). The results are compared to that of a particle-doped case with corresponding filling factors $1 - f$ (shown by the dashed lines). With the same strength, adiabatic doping is more efficient in the hole-doped regime compared to the particle-doped regime.

potential strength, which means the breakdown of adiabatic preparation corresponds to the atom localization. The results are compared to that in a particle-doped regime with $f = [\sqrt{5} - 1]/2$ (approximated by 55/89) and $\mathcal{V} = 8E_R$. For most of the Hamiltonian evolution path, the IPR of hole doping is smaller than that of particle doping, especially for $s > 0.5$ where the strength of the final potential becomes dominant. This is because in comparison with the particle-doping case, the final lattice constant is smaller for hole doping, for which quantum tunneling is stronger, suppressing the atom localization. The quantum adiabatic doping protocol is evidently more efficient in the case of hole doping than particle doping.

B. Interacting fermion

We further consider adiabatic hole doping of interacting fermions, and simulate the evolution process starting from

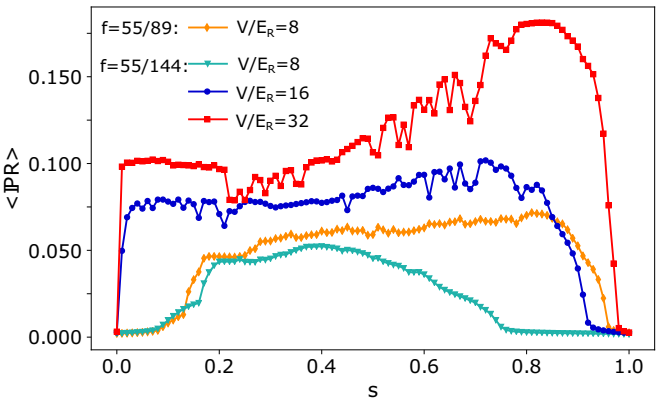

FIG. 7. Averaged inverse participation ratio (IPR) along the evolution path with $\mathcal{V} = 8E_R, 16E_R, 32E_R$ in the hole-doped regime and $\mathcal{V} = 8E_R$ in the particle-doped regime. In the calculation, the IPR is averaged over the lowest L single-particle eigenstates of one spin component. The filling factor is set to be $f = [3 - \sqrt{5}]/2$ and $f = [\sqrt{5} - 1]/2$ that are approximated by a Fibonacci sequence as F_{n-2}/F_n and F_{n-2}/F_{n-1}, respectively, with an initial lattice size $L = 55$. Compared to particle doping, the IPR for hole doping is smaller for most of the evolution path, which explains the high preparation efficiency in this regime.

a one-dimensional interacting band insulator using DMRG. We choose $f = 2/5$ with $L = 12$ for the rational filling and $f = [3 - \sqrt{5}]/2$ for the irrational one, which is approximated by $f = 13/34$ with $L = 13$ in the calculation. The dependence of the final-state wave-function overlap and residual energy per particle on the interaction strength is shown in Fig. 8 (solid lines) with an overall potential strength $\mathcal{V} = 8E_R$. The DMRG calculation shares the same time sequence and parameter choice with that in the particle-doped regime. Two choices of the total evolution time, $T = 50\hbar/E_R$ and $T = 200\hbar/E_R$, are considered. The preparation efficiency is improved by introducing a strong atomic interaction. In our numerical results, we find a systematic increase of the wave-function overlap [Eq. (8)] and a reduction of residual energy with increasing interaction strength. By increasing the interaction strength g from 0 to 0.6 (in units of λE_R), the wave-function overlap ultimately reaches 0.96 for $f = 13/34$ and 0.965 for $f = 2/5$. We compare the results with that of particle doping (dashed line) for the same interaction and confinement potential strengths. As shown in Fig. 8(c), the wave-function overlap with $T = 50\hbar/E_R$ in the hole-doped regime is even larger than that of particle doping with $T = 200\hbar/E_R$. The hole doping is evidently more efficient than the particle doping in the interacting regime, as is true for the noninteracting case as well.

V. CONCLUSION

To conclude, the doped quantum phase of an atomic Fermi-Hubbard model with low thermal entropy can be prepared by adiabatically converting two optical lattices with different spatial periods. In this adiabatic doping proposal, an arbitrary filling fraction can be achieved by choosing the lattice constant ratio of the initial and final lattices. In this work, we consider quantum adiabatic doping starting from a band insulator in a one-dimensional lattice and systemically study

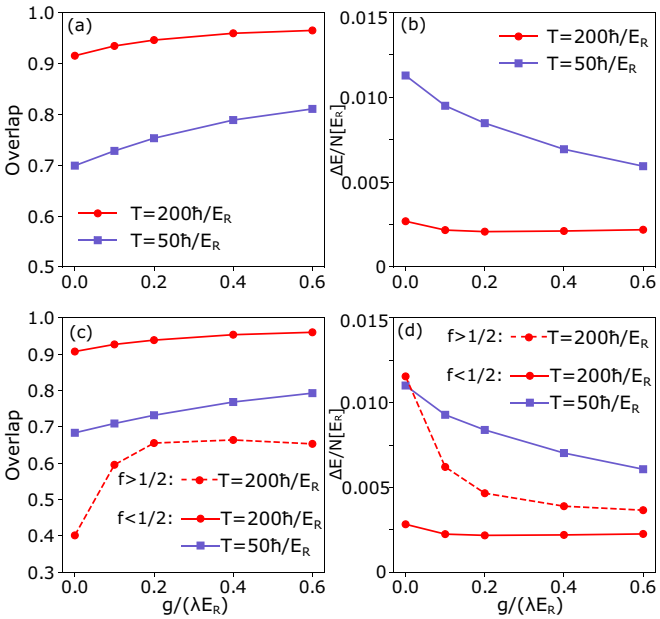

FIG. 8. Performance of adiabatic hole doping of interacting fermions in a one-dimensional lattice for both rational and irrational fillings. The wave-function overlap and residual energy per particle are shown with solid lines in (a), (b) for $f = 2/5$ with $L = 12$ and (c), (d) for $f = [3 - \sqrt{5}]/2$, which is approximated by $13/34$ with $L = 13$. Here, we consider the total adiabatic time $T = 50\hbar/E_R$ and $T = 200\hbar/E_R$. The overall potential strength is $\mathcal{V} = 8E_R$ for both particle and hole doping. As we increase the interaction strength, the wave-function overlap increases and approaches 1 for $T = 200\hbar/E_R$, and the residual energy is reduced accordingly. Compared to particle doping (shown by dashed lines with a filling factor $f = 13/21$), hole doping shows a better preparation efficiency for this interacting case.

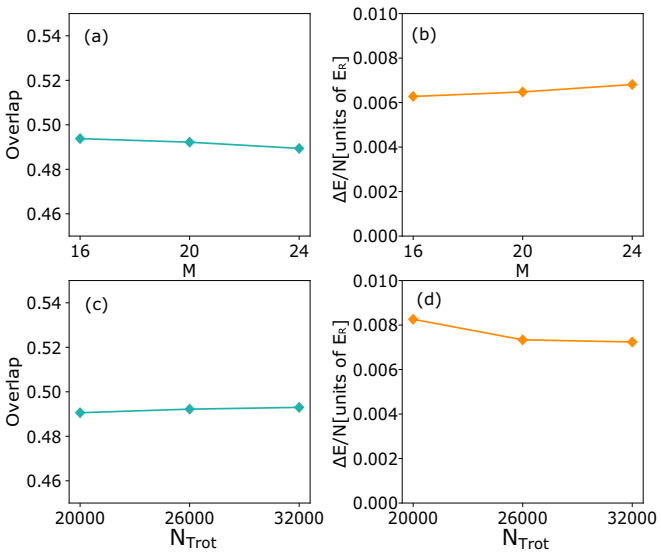

FIG. 9. The convergence of results of a wave-function overlap [Eq. (8)] and the residual energy [Eq. (9)] in the DMRG calculation. We simulate the adiabatic doping of one-dimensional interacting fermions with the same parameter choice as in Fig. 4 and fixed interaction strength $g = 0.2\lambda E_R$. Additional numbers of grids [shown in (a), (b)] and numbers of Trotter steps [shown in (c), (d)] are considered.

the proposal for a broad range of filing fractions from particle doping to hole doping, including both rational and irrational cases. It is found that atom localization, which is a fundamental problem in incommensurate lattices, also prevents efficient adiabatic doping for a commensurate filling at strong lattice confinement. Through a DMRG simulation, we show that localization is suppressed by introducing a strong atomic interaction and the state preparation efficiency is consequently improved. Compared to particle doping, adiabatic hole doping is more efficient in both free and interacting regimes. We also consider adiabatic doping starting from a Mott insulator state at half filling. From the results of a DMRG calculation, we find that this protocol has significantly higher preparation efficiency than adiabatic doping starting from a band insulator for a certain range of filling factors.

Although the numerical simulation of the quantum adiabatic doping process is restricted to one dimension in this work due to numerical cost, we anticipate a better performance in two dimensions because the localization physics is largely expected to be weaker in higher dimensions. Our systematic study of different fillings and interaction effects should also shed light on quantum adiabatic doping in two dimensions.

ACKNOWLEDGMENTS

This work is supported by National Key R&D Program of China (under Grants No. 2018YFA0306502 and No. 2017YFA0304204), National Natural Science Foundation of China (Grants No. 11934002 and No. 11774067), National Program on Key Basic Research Project of China (Grant No. 2017YFA0304204), Shanghai Science Foundation (Grant No. 19ZR1471500), and the Open Project of Shenzhen Institute of Quantum Science and Engineering (Grant No. SIQSE202002). Calculations were performed based on the ITensor Library [47].

APPENDIX: DETAILS OF DMRG SIMULATION

Here, we provide numerical details of our DMRG simulation. In discretizing the continuous degrees of freedom of interacting fermions, each spatial period of the initial lattice is divided into $M = 20$ grids, if not specified. The numbers of total Trotter steps are $N_{\text{Trot}} = 7000$, 26 000, 38 000, and 50 000 for the total evolution time $T = 50\hbar/E_R$, $200\hbar/E_R$, $300\hbar/E_R$, and $400\hbar/E_R$, respectively. The corresponding Trotter step is $\tau \leqslant 0.008\hbar/E_R$. In Fig. 9, we calculate the ground states and simulate the time evolution of interacting fermions with the same parameter choice as in Fig. 4, and check the convergence with increasing the number of discretization grids, and Trotter steps, i.e., M and N_{Trot}. In the calculation, the interaction strength is set to be $g = 0.2\lambda E_R$. As M is increased from 16 to 24, we only see a minor variation for both the wave-function overlap [Eq. (8)] and the residual energy [Eq. (9)]. Similarly for Trotter steps increasing from 20 000 to 32 000, we also find a nice convergence in the overlap and the residual energy.

[1] I. Bloch, J. Dalibard, and W. Zwerger, Rev. Mod. Phys. **80**, 885 (2008).
[2] X. Li and W. V. Liu, Rep. Prog. Phys. **79**, 116401 (2016).
[3] M. Lewenstein, A. Sanpera, V. Ahufinger, B. Damski, A. Sen, and U. Sen, Adv. Phys. **56**, 243 (2007).
[4] I. Bloch, Nat. Phys. **14**, 1159 (2018).
[5] D. Jaksch, C. Bruder, J. I. Cirac, C. W. Gardiner, and P. Zoller, Phys. Rev. Lett. **81**, 3108 (1998).
[6] W. Hofstetter, J. I. Cirac, P. Zoller, E. Demler, and M. D. Lukin, Phys. Rev. Lett. **89**, 220407 (2002).
[7] O. Dutta, M. Gajda, P. Hauke, M. Lewenstein, D.-S. Lühmann, B. A. Malomed, T. Sowiński, and J. Zakrzewski, Rep. Prog. Phys. **78**, 066001 (2015).
[8] P. A. Lee, N. Nagaosa, and X.-G. Wen, Rev. Mod. Phys. **78**, 17 (2006).
[9] W. Metzner, M. Salmhofer, C. Honerkamp, V. Meden, and K. Schönhammer, Rev. Mod. Phys. **84**, 299 (2012).
[10] H.-C. Jiang and T. P. Devereaux, Science **365**, 1424 (2019).
[11] M. Qin, C.-M. Chung, H. Shi, E. Vitali, C. Hubig, U. Schollwöck, S. R. White, and S. Zhang (Simons Collaboration on the Many-Electron Problem), Phys. Rev. X **10**, 031016 (2020).
[12] D. Greif, T. Uehlinger, G. Jotzu, L. Tarruell, and T. Esslinger, Science **340**, 1307 (2013).
[13] R. A. Hart, P. M. Duarte, T.-L. Yang, X. Liu, T. Paiva, E. Khatami, R. T. Scalettar, N. Trivedi, D. A. Huse, and R. G. Hulet, Nature (London) **519**, 211 (2015).
[14] A. Mazurenko, C. S. Chiu, G. Ji, M. F. Parsons, M. KanÃ¡sz-Nagy, R. Schmidt, F. Grusdt, E. Demler, D. Greif, and M. Greiner, Nature (London) **545**, 462 (2017).
[15] J. Lin, J. Nan, Y. Luo, X.-C. Yao, and X. Li, Phys. Rev. Lett. **123**, 233603 (2019).
[16] S. Trebst, U. Schollwöck, M. Troyer, and P. Zoller, Phys. Rev. Lett. **96**, 250402 (2006).
[17] A. S. Sørensen, E. Altman, M. Gullans, J. V. Porto, M. D. Lukin, and E. Demler, Phys. Rev. A **81**, 061603(R) (2010).
[18] M. Lubasch, V. Murg, U. Schneider, J. I. Cirac, and M.-C. Banuls, Phys. Rev. Lett. **107**, 165301 (2011).
[19] Z. Zhang and L.-M. Duan, Phys. Rev. Lett. **111**, 180401 (2013).
[20] C. S. Chiu, G. Ji, A. Mazurenko, D. Greif, and M. Greiner, Phys. Rev. Lett. **120**, 243201 (2018).
[21] H. Sun, B. Yang, H.-Y. Wang, Z.-Y. Zhou, G.-X. Su, H.-N. Dai, Z.-S. Yuan, and J.-W. Pan, arXiv:2009.01426.
[22] S. Iyer, V. Oganesyan, G. Refael, and D. A. Huse, Phys. Rev. B **87**, 134202 (2013).
[23] M. Schreiber, S. S. Hodgman, P. Bordia, H. P. Lüschen, M. H. Fischer, R. Vosk, E. Altman, U. Schneider, and I. Bloch, Science **349**, 842 (2015).
[24] J. C. C. Cestari, A. Foerster, M. A. Gusmão, and M. Continentino, Phys. Rev. A **84**, 055601 (2011).
[25] V. P. Michal, B. L. Altshuler, and G. V. Shlyapnikov, Phys. Rev. Lett. **113**, 045304 (2014).
[26] A. Lukin, M. Rispoli, R. Schittko, M. E. Tai, A. M. Kaufman, S. Choi, V. Khemani, J. Léonard, and M. Greiner, Science **364**, 256 (2019).
[27] M. Rispoli, A. Lukin, R. Schittko, S. Kim, M. E. Tai, J. Léonard, and M. Greiner, Nature (London) **573**, 385 (2019).
[28] T. Kohlert, S. Scherg, X. Li, H. P. Lüschen, S. Das Sarma, I. Bloch, and M. Aidelsburger, Phys. Rev. Lett. **122**, 170403 (2019).
[29] J. Smith, A. Lee, P. Richerme, B. Neyenhuis, P. W. Hess, P. Hauke, M. Heyl, D. A. Huse, and C. Monroe, Nat. Phys. **12**, 907 (2016).
[30] P. Roushan, C. Neill, J. Tangpanitanon, V. Bastidas, A. Megrant, R. Barends, Y. Chen, Z. Chen, B. Chiaro, A. Dunsworth, A. Fowler, B. Foxen, M. Giustina, E. Jeffrey, J. Kelly, E. Lucero, J. Mutus, M. Neeley, C. Quintana, D. Sank *et al.*, Science **358**, 1175 (2017).
[31] K. Xu, J.-J. Chen, Y. Zeng, Y.-R. Zhang, C. Song, W. Liu, Q. Guo, P. Zhang, D. Xu, H. Deng, K. Huang, H. Wang, X. Zhu, D. Zheng, and H. Fan, Phys. Rev. Lett. **120**, 050507 (2018).
[32] T. Albash and D. A. Lidar, Rev. Mod. Phys. **90**, 015002 (2018).
[33] S. R. White and A. E. Feiguin, Phys. Rev. Lett. **93**, 076401 (2004).
[34] A. E. Feiguin and F. Heidrich-Meisner, Phys. Rev. B **76**, 220508(R) (2007).
[35] A. Lüscher, R. M. Noack, and A. M. Läuchli, Phys. Rev. A **78**, 013637 (2008).
[36] M. Tezuka and M. Ueda, Phys. Rev. Lett. **100**, 110403 (2008).
[37] M. Rizzi and A. Imambekov, Phys. Rev. A **77**, 023621 (2008).
[38] R. Bell and P. Dean, Discuss. Faraday Soc. **50**, 55 (1970).
[39] D. Weaire and A. Williams, J. Phys. C **10**, 1239 (1977).
[40] D. Weaire and V. Srivastava, J. Phys. C **10**, 4309 (1977).
[41] D. Weaire and V. Srivastava, Solid State Commun. **23**, 863 (1977).
[42] T. Odagaki, Solid State Commun. **33**, 861 (1980).
[43] F. Wegner, Z. Phys. B **36**, 209 (1980).
[44] J. Biddle, B. Wang, D. J. Priour, and S. Das Sarma, Phys. Rev. A **80**, 021603(R) (2009).
[45] J. Biddle, D. J. Priour, B. Wang, and S. Das Sarma, Phys. Rev. B **83**, 075105 (2011).
[46] X. Li, X. Li, and S. Das Sarma, Phys. Rev. B **96**, 085119 (2017).
[47] ITensor Library (version 2.0.11), http://itensor.org.